

Optical manipulation: a step change for biomedical science

Carl A. Campugan^{1,2}, Kylie R. Dunning^{1,2,3} and Kishan Dholakia^{3,4,5,6, *}

¹Robinson Research Institute, Adelaide Medical School, The University of Adelaide, Adelaide, South Australia, Australia,

²Australian Research Council Centre of Excellence for Nanoscale BioPhotonics, The University of Adelaide, Adelaide, South Australia, Australia

³Institute for Photonics and Advanced Sensing, The University of Adelaide, Adelaide, South Australia, Australia

⁴School of Physics and Astronomy, University of St Andrews, North Haugh, Scotland KY16 9SS

⁵School of Biological Sciences, The University of Adelaide, Adelaide, South Australia, Australia

⁶Department of Physics, College of Science, Yonsei University, Seoul 03722, South Korea

*Corresponding author: Kishan Dholakia, kd1@st-andrews.ac.uk

Twitter: @OpticManip (KD); @DrKylieDunning (KRD)

ORCID for all authors:

0000-0003-4947-8251 (CC), 0000-0002-0462-6479 (KRD), 0000-0001-6534-9009 (KD).

Optical manipulation: a step change for biomedical science

Abstract

The transfer of optical momentum can exert miniscule but important forces on biological specimens. This area of optical manipulation has been thriving for over fifty years. Its importance was recognised by the award of half of the Nobel Prize in Physics in 2018 to Arthur Ashkin for the use of a single focused light beam for manipulation, namely optical tweezers. This article reviews the basic physics of trapping and gives an overview of the basic premise of the field. We particularly focus upon its importance and impact for the biomedical sciences.

Keywords: optical tweezers; optical trap; biophysics

1 Introduction

In Physics, light holds a special place. Its invariance of speed in different frames of reference is key to understanding relativity. In the standard model it mediates the electromagnetic interaction. Importantly, the photon—the quantum of electromagnetic radiation—possesses momentum. Einstein's famous experiment on the photoelectric effect in 1905 was a clear indicator of the concept of light comprising of quantised units of energy, the photon. This was followed by the famous Compton effect experiment in 1922 that conclusively showed that a photon carried momentum proportional to its wave number.

The history of the momentum of light exerting a force goes back to the 16th Century, to the German astronomer, Peter Apian. In 1531, he illustrated his observations in careful hand-coloured drawings showing the tail of Halley's Comet extending away from the sun. Johannes Kepler followed up with further thoughts for the origins of the behaviour of comet tails. In 1619 he published his view on why the tails of comets, on their highly eccentric orbits, point away from the sun. To explain his observations, Kepler invoked the notion of solar light pressure—a radical notion signifying the basis that light could exert a force. The solar

interaction with such a celestial object led Kepler to believe that a space sail might one day harness sunlight, in the same manner as the sail of a boat captures the wind.

The concept of electromagnetic radiation was developed and at the beginning of the 20th century. Nichols and Hull performed a key study of the radiation pressure of light being exerted on a macroscopic object. James Clerk Maxwell had calculated stresses in the electromagnetic field and predicted this outcome in 1873. Based on a thermodynamics viewpoint, Adolpho Bartoli also predicted the effect in 1876. Nichols and Hull circumvented shortcomings of previous attempts, due to residual gases, incorporating both the ubiquitous gas heating and ballistic effects in such a system and in this way, verified Maxwell's theory [1,2]. A separate demonstration was undertaken at that time by Pyotr Lebedev at Moscow State University in Russia [3].

Whilst important, it took a landmark discovery in optics to make a step change for optical forces: in 1960 Theodore Maiman invented the first laser, heralding a step change in the use and application of light. In the 1960s Arthur Ashkin and others started investigating the light-matter interaction in new ways, aiming to utilise of optical forces across a wide range of the sciences. This force is a result of the change of the momentum of light with matter. However, this momentum p , given by the famous de Broglie relation $p = h/\lambda$ (where λ is the wavelength and h is Planck's constant), is miniscule: for a photon of visible wavelength it is around 10^{-27} kgms⁻¹. However, at the mesoscopic scale (nanometre to micrometre size), the mechanical effects of optical fields have made a significant impact that is not restricted to biological material. They have given key insights into fundamental physics, colloidal science, chemical interactions and beyond, showing its immense reach across the sciences.

In this review, we will focus upon the impact of optical forces for biomedicine. Ashkin was the key pioneer of the field of optical manipulation for mesoscopic particles. He was also passionate about trapping atoms with light which has emerged separately as a major field with

impact in atomic and quantum physics. Optical manipulation has seen unprecedented expansion in the last five decades, culminating in the award of half of the Nobel Prize in Physics in 2018 to Ashkin for his work and its impact on biology. It is this latter aspect which forms the focus of this review. We note optical tweezers has made an exceptionally widespread impact across all the sciences, enhancing our understanding of the light-matter interaction, the nuances of structured light, nonequilibrium thermodynamics and even inroads into optomechanics. We are not able to cover all these topics here and refer the interested reader elsewhere [4-7]. To date, the biomedical sciences has perhaps seen the most significant impact with optical traps and this is the key topic of this article. We begin with discussion of the basic geometries developed from a physics standpoint covering the main types of optical traps. We mention the theoretical modelling that can be applied to understand the forces on a trapped particle and then progress to focus on how this can be tailored to measure force and displacement accurately, a crucial aspect for the biological sciences. We then elucidate how optical manipulation can be used for answering key questions for single molecule biophysics, cellular studies and *in vivo* applications.

2 The Development of Optical Manipulation and Optical Tweezers

Ashkin's first study used micron-sized spheres manipulated with a visible wavelength laser source [8]. Sending the laser beam in horizontally into a liquid sample medium, aligned these microspheres with the beam propagation axis. These microspheres were then seen to be propelled along the laser beam direction due to radiation pressure. This was the first demonstration of optical guiding: the relay of particles along the bright centre of a propagating light beam [8]. This may be understood as follows: the optical force from the gradient of the light field draws the object into the beam axis and a radiation pressure (scattering) component propels the particle along the beam propagation axis. This is the case for particles of higher refractive index than that of their surroundings. Ashkin added a second counterpropagating

light beam (of the same power) creating a radiation pressure force in the opposite direction. Under these conditions, the particle came to rest between the two laser beams, realising the first optical trap. This was the so-termed counter propagating dual-beam trap geometry [8]. Using single-mode optical fibers rather than free space optics makes this dual-beam trap system more practical [9]. In itself, the counterpropagating beam trap is important for the biomedical sciences and we shall discuss its particular attributes later in this article.

A milestone was reached in 1986: Ashkin and colleagues demonstrated how one light field could confine a particle using the single-beam gradient trap, known as optical tweezers [10]. This is cemented as the most widely used method for applying optical forces to hold and manipulate microscopic particles. Such optical tweezers are compatible with a standard microscope and may be implemented solely using a microscope objective with a high numerical aperture above unity. The laser powers needed are not high and of the order of a few mW per trap site, but due to the tight focusing may lead to high power densities leading to potential heating issues, which we shall discuss later.

From these early studies, optical manipulation has seen a consistent and ever-increasing impact across a variety of different fields. Although there are also several recent review papers in the general field of trapping, this paper focuses upon the impact of optical traps in biomedicine, namely cell biology, *in vivo* studies and for single-molecule biophysics, bringing to the fore the physical aspects that have underpinned these studies. This paper is organised as follows: First, we describe the theoretical basis for single-beam optical trapping, including a discussion of how the forces may be understood to operate at different size scales. We then progress to describe experiments related to single molecule studies and cell biology. We include a discussion of laser damage and heating and conclude with advanced topics in trapping and the combination of trapping with other methodologies. Our aim is not to give a comprehensive overview but rather highlight the important physics innovations in optical

manipulation used for biomedical discovery. We conclude with a brief discussion on the future applications of optical manipulation for the life sciences.

3 Theoretical Basis for Optical Trapping

Optical manipulation is a generic phrase widely used to cover the breadth of application of the forces of light to transport and trap mesoscopic sized objects in both two and three dimensions. Optical tweezers uses a single tightly focused beam to optically trap particles in 3D and is based on an inhomogeneous optical field distribution. In addition to scattering or refraction, laser light may be absorbed in the sample medium, trapped particle or biological specimen, resulting in thermal forces. These can often overwhelm optical forces and as such due care needs to be taken. Optical trapping is thus constrained to relatively transparent media and particles where any thermal effects are negligible. For biomedical studies, any optically induced changes in temperature can adversely affect biological viability. This may be circumvented with judicious choice of trap laser wavelength and other parameters. We shall discuss this aspect later on in this review.

The dimensions of the trapped particle (of radius r) and those of the wavelength of the trapping laser source (λ) determines how we consider the light-particle interaction and the resultant optical forces. For the case of a dielectric particle where $r \ll \lambda$, the particle may be treated an oscillating dipole, and is the so-termed Rayleigh limit. In this limit we may consider the optical force comprising of a gradient force F_g and scattering force F_s . The scattering force is proportional to the intensity gradient of the optical field (I), $F_s \propto I$. The gradient force is proportional to the polarizability α of particle and field intensity, $F_g \propto \alpha \nabla I$. This relation explains why it can be challenging to trap dielectric particles below a micron in diameter as α is proportional to particle volume. This relation also explains why though very small dielectric particles (e.g. $r \sim 100\text{nm}$) are challenging to trap, in fact metallic nanoparticles may be readily

confined, being highly polarisable. The complex nature of the refractive index of a metallic particle needs consideration as this may result in appreciable thermal effects.

For the converse case where the particle size significantly surpasses the wavelength of the trapping light, i.e. $r \gg \lambda$, the geometrical (ray) optics formalism is appropriate. This is perhaps the most evocative and accessible way to understand the operation of optical tweezers. Here the propagation of light through the trapped sphere is determined through the principles of simple ray propagation and the use of Snell's law at the interfaces between the particle and the medium. The reflection and refraction of light at the boundary of the trapped particle may be used to determine the forces exerted. Figure 1 describes how a dielectric particle may be trapped by a single focused beam: i.e. in optical tweezers. A particle of higher refractive index than its surroundings is drawn into the most intense part of the optical field. We may consider the beam as a set of individual rays, each with weighted intensity matching the beam profile and propagating in a sample medium of refractive index n . Each individual ray alters direction upon reflection or refraction as it is incident on the particle with the ray path dictated by the Fresnel equations. These result in forces to confine the particle very close to beam focus (Figure 1). For a Gaussian trapping beam, we create a parabolic potential well (over a given distance from trap centre). Such a potential leads to a linear relationship between force and extension (Figure 1c) near trap centre with the force becoming independent of position at the periphery of the beam before falling rapidly at more extended distances. This force vs position dependency is used in studies in biomedicine, as we shall see later.

[Figure 1 near here]

Experiments are often conducted with trapped particles of a size comparable to the trapping laser wavelength ($r \sim \lambda$). Such particles turn out to be near optimal for obtaining the maximum trap stiffness with lowest error in force measurements [11]. In this case, classical

electrodynamics is required to understand the behaviour. The force exerted on an object positioned in a time-harmonic electromagnetic field may be calculated using the law of conservation of linear momentum. The linear momentum in this instance is either within the optical field or is present as mechanical momentum of the particle. The sum of these two parts, which is the total momentum of the system, is conserved. The electromagnetic field momentum flux in a linear medium of relative permittivity ϵ_m and permeability μ_m is represented mathematically by the Maxwell stress tensor. The optical force expressed in these terms is of general validity for an arbitrary (albeit rigid) body within the surface. It is entirely determined by the electric and magnetic fields at the surface [12]. When considering deformable objects (such as a cell), both electrostrictive and magnetostrictive forces have to be considered. This approach is very general and powerful and may in fact be applied for all ratios of particle size to trapping wavelength if desired.

We also remark that the force field in optical tweezers shows both a conservative and non-conservative component: the gradient force is conservative and may be related to a potential, whereas the scattering force is non-conservative and dissipative. It is not possible to relate this to an effective potential. Its influence on particle position fluctuations is in fact to create toroidal vortex trajectories [13]. The non-conservative component to the force adds intriguing physics to optical traps but is not a major consideration for calibrating and using optical tweezers for biomedicine.

4 Measuring Force in Optical Traps

Overall, optical tweezers for trapping in liquid media may be modelled as an overdamped simple harmonic oscillator. The power of optical tweezers centres upon its ability to measure the force exerted on a trapped particle and record its position variation with time. Optical tweezers acts as a Hookean spring: the force F is proportional to the displacement (x) of the

sample from equilibrium $F = -k_{trap}x$, with the constant of proportionality being the trap stiffness (k_{trap}). This assumption is valid for up to around 200nm or so around the centre of the optical trap. Measuring sample position may thus eventually be used to calculate the force if the system is calibrated. A prerequisite, however, is that this must be performed at nanometre and millisecond accuracy and naturally should be reproducible. Three key methods have emerged in this regard for determining trap stiffness: the drag method, the use of energy equipartition and the use of the power spectrum. We refer the reader elsewhere for a detailed discussion and comparison between these approaches which have their own attributes and drawbacks [4]. The power spectrum approach has proved popular for biomedical studies: a position histogram is recorded by imaging the trapped particle onto a quadrant photodiode. Taking the Fourier transform of particle position yields a Lorentzian-shaped power spectrum, where the roll off frequency is related to the trap stiffness. Knowing the Stokes drag on the particle, and assuming a linear relation between particle displacement and detector voltage, are prerequisites for this approach.

For the case of many single molecule studies, just operating in the linear region of the trap (a few hundred nm around trap centre) is not enough, as in fact we have two attached springs to consider: one of the trapped particle and the other of the molecule itself. As an example, we may consider the case for DNA adhered to an enzyme on a slide, with its other end adhered to a microparticle. Motion of the enzyme alters the extension of the DNA with the movement of the particle restricted by the trap stiffness. Overall, the result is the motion of the particle is not the same as motion of the molecule under investigation, complicating the analysis. To tackle this limitation some innovative methods were developed. A key advance was operating at the point of trap stiffness (k_{trap}) being zero. This does not equate to a force of zero but means we are operating at a point with constant force for a range of particle displacement (see Figure 1c). This optical force clamp avoids the need to incorporate the

compliance of the biological molecule in studies. For a constant applied force, the biological link does not vary its extension [14].

New concepts and approaches are also emerging for this area to obviate the need for frequent calibration of the trap, which may be deleterious for experimental studies. In particular measuring the change in momentum between the incoming and outgoing light is emerging as an alternative way to look at this issue. This is not related to the specific trapping beam, particle size or particle shape [15,16]. This concept has been advanced recently to deduce individual forces for several optical traps simultaneously using the multiplexing afforded by holographic tweezers for force measurements [17]. This opens up the possibility of quantitative multipoint force measurements in complex biological settings (e.g. cell flow in the blood stream). Other notable recent work has seen the emergence of a novel route to reconstruct the microscopic force using a maximum-likelihood-estimator analysis (termed FORMA). The method may rapidly determine both conservative and non-conservative components of the force field. Such analysis may be useful for future optical traps and their use as microscopic and nanoscopic force transducers [18].

5 Molecular motors

The existence of molecular motors was first reported in 1864. Since then, a plethora of studies have led to a better understanding of the role molecular motors play in cellular function. These motors utilise chemical energy to fuel mechanical work within cells and fall within three categories:

- (1) *Cytoskeleton motor proteins*, including kinesin, myosin and dynein. These are linear motors that bind to and transit along the cytoskeleton, a network of microtubule and actin filaments spread throughout a cell. These are involved in muscle contraction, cellular transport and the segregation of chromosomes during cell division. These

motor proteins are composed of two domains, the two-headed motor domain that transits along the cytoskeleton track in a 'hand-over-hand' fashion, a process akin to walking, and the 'cargo binding' domain that specifies the type of cargo it transports. Cytoskeleton motor proteins are fuelled by the hydrolysis of adenosine triphosphate (ATP) to adenosine diphosphate (ADP).

(2) *Nucleic acid motor proteins*, including DNA and RNA polymerases. These motor proteins bind DNA and RNA and are critically important for the maintenance of genetic code and for the production of all proteins within cells. Energy to fuel these motor proteins comes from polymerisation of nucleic acids, protein synthesis and/or hydrolysis of ATP to ADP. Our understanding of these motors is far less complete compared to cytoskeleton motor proteins, likely due to the complex nature of these biological processes.

(3) *Rotary motor proteins*, namely F₀F₁-ATP synthase, which synthesises cellular energy in the form of ATP and flagella, which are necessary for the movement of bacteria. These motors are embedded within cell membranes and produce torque through mechanical rotation and are powered by electrochemical potential, a proton or sodium ion gradient. As with nucleic acid motor proteins, we know less informed as to their function, compared to the case of cytoskeleton motor proteins.

The importance of molecular motors is best illustrated where mutations result in an altered function and consequently, disease. Examples include deafness (mutations in myosin VI); infertility (dynein); cardiomyopathy (cardiac myosin); and neurodegenerative diseases (kinesin). Before the advent of optical tweezers, knowledge of molecular motor function and associated pathologies was achieved using an array of *in vitro* assays. However, these were limited in their capability to quantify force and motion. This is where optical tweezers have made a significant impact.

5.1 Optical tweezers to study molecular motors—manipulating single molecule biophysics

Our understanding of muscle contraction (e.g., energy consumption, contraction rate) had until recently come from bulk *in vitro* assays using muscle fibers. Single-molecule experiments using optical tweezers have advanced this field over the last three decades, enabling direct measurement of individual motors and answering questions such as: do they move in discrete, regular steps? Do they pause? How big is the step size? What force do they exert? We now know that molecular motor proteins act in a distinct, stepwise manner with high efficiency. The study of different molecular motors necessitates the use of an array of optical tweezers assays (Table 1) (Figure 2), tailored to accurately measure force (at the piconewton level) and displacement (nanometre to Ångstrom scale).

[Table 1 & Figure 2 near here]

Cytoskeletal motor proteins: kinesin, dynein and myosin

The most frequently used optical tweezers geometry for measuring the force of a molecular motor is shown in Figure 2a. In this design, motor proteins or a single microtubule are tethered to a particle, usually polystyrene or silica (typically $\sim 1 \mu\text{m}$ in diameter), via chemical binding (creation of a biotin-streptavidin link) [19]. The fixed surface is prepared in the opposite manner, by the binding of a microtubule or motor protein, respectively. The particle is then optically trapped, enabling manipulation of single molecules attached to the bead. The force applied by the trap can then be used to stall or slow the molecular motor kinesin, enabling measurement of both force and velocity and their relationship [20,21]. To measure kinesin and dynein generated forces, the bead is displaced from the centre of the trap due to the motility of the molecular motor, until a point where the bead snaps back to the trap centre. This occurs

due to the stalling of the molecular motor (stall force) and its displacement from the microtubule [22,23]. Measuring these stall forces provides information on the type of load the motor protein is capable of transporting as well as conditions that affect its function (e.g. temperature and availability of chemical energy; ATP) [24,25]. This stall force may also be determined using zero-velocity plateaus before snap-back occurs [21,26]. Alternatively, measurement of stall force is achieved by lowering the force of the trap until a point where the molecular motor resumes [27].

Force clamps, which we discussed earlier are where the optical trap applies constant force (see Figure 2b). They are useful in measuring step size and isometric stall force [21,28]. Here the trap maintains the same trapping position of the kinesin coated particle by responding to the movement of the motor. This geometry can also be used to apply an external force, stimulating kinesin and dynein to commence stepping/motility [28,29]. This external force can stimulate dynein to commence stepping unidirectionally along a microtubule, as occurs within a cell. While kinesin naturally transits in a forward direction along a microtubule track, an external backward load applied by a force clamp can remarkably stimulate stepping in a backward direction.

Collectively, these studies showed that kinesin advances in discrete 8nm steps, with binding and hydrolysis of an ATP molecule required at each step. Further, these motors also show a stall force of 5-7 pN. For dynein, reported step size varies from 8–32 nm, dependant on force load [30]. This extraordinary work demonstrates the power of optical tweezers to measure small changes in the biomechanics of kinesin and dynein and directly links the work performed by the motor specifically to these chemical reactions.

Due to its unique mechanism of action, a different optical tweezers assay is required to study myosin (Figure 2c) [31]. Here, a silica particle is attached to a fixed surface (coverslip) in order to raise a single myosin molecular motor, allowing it to come in contact with an actin

fibre. The actin fibre is suspended between two particles, each individually held in a separate optical trap. As myosin interacts and moves along the actin track, force of motion can be quantified based on tension and displacement detected by the trapped beads. This tweezers assay has enabled characterisation of myosin step biomechanics including step size (11 nm), step force (3-6 pN), attachment distance (~40 nm) and travel distance (~5-10 steps prior to load detachment) [31-33].

Nucleic acid motor proteins: RNA polymerase as an example

The RNA polymerases are responsible for transcribing DNA into RNA, an essential intermediary step in the translation of genetic code into protein, also known as gene expression. Transcription involves opening double stranded DNA and threading the separated strands through RNA polymerase. The enzyme then moves along the DNA template, in a stepwise manner, transcribing genetic code into a complementary single stranded messenger RNA. Single molecule experiments with optical tweezers have significantly advanced our knowledge of the biomechanics of RNA polymerases, which work on the smaller ångström level compared to the nanometer scale of kinesin and dynein molecular motors.

The stall force for RNA polymerase was shown to range from ~21-27 pN [34], considerably greater than the ~5-7 pN determined for kinesin. This may reflect the requirement for RNA polymerase to separate the entangled DNA structure. This work and other studies show that RNA polymerase pauses for periods of 0-30 seconds (measured at ~100 ms scale), necessary for the protein to backtrack as few as 2 base pairs (~7 Å) to proofread what is already transcribed [35,36]. More recently, the step size of RNA polymerase was determined by Abbondanzieri et al. [37]. In this study the authors describe an ultra-stable, dual beam optical tweezers assay (Figure 2d). Importantly, this advance allowed a step from nanometre to ångström level position resolution in optical tweezers, crucial to resolve the minute steps taken by *E. coli* RNA polymerase during transcription. Normal force clamps may suffer from

variations in signal fluctuations and beam pointing stability of the laser trap. One key part to overcome these issues was to place the optics external to the microscope in a chamber filled with helium gas rather than air. As the refractive index of helium was around an order of magnitude closer to vacuum than air, the pointing stability of the optical beam was reduced by the same level yielding an instrument with angstrom-level stability. A further important piece of physics was the use of a passive force clamp by using a bead placed at the turnover point in the force vs extension curve as described earlier (Figure 3 and see also Figure 1c). This obviated the need for computational correction of forces. In tandem, this led to a deeper understanding of transcription, showing that RNA polymerase has a discrete step size of $3.7 \pm 0.6 \text{ \AA}$, consistent with the size of one base pair of DNA [37].

[Figure 3 near here]

DNA elasticity – pulling experiments

Within cells, DNA is stretched, twisted and bent in biological processes like transcription, as described above. In pioneering studies, optical tweezers have been used to stretch DNA to better understand its elastic properties and thus how it withstands the mechanical stress of various cellular processes [38,39]. In so called pulling experiments, single beam traps have been used where the DNA strand is tethered between an optically trapped particle and a fixed surface (coverslip) or pipette. The distance between the bead and coverslip, or pipette, is increased in order to apply increasing force/stretch. The extension of DNA under increasing force is recorded and presented as a force to extension (FE) curve. These studies show that DNA, when in its right-hand double helix configuration, has elastic characteristics that are entropic in nature when forces are below 5 pN. This elastic behaviour is best described by the worm-like chain (WLC) model which works under the assumption that DNA is a flexible rod of a particular length. When a force beyond 10 pN is applied the behaviour of DNA becomes

intrinsic due to a change in DNA structure/confirmation. Interestingly, at ~65 pN DNA undergoes the *overstretching transition* when a conformational change in structure (where the helix partially unwinds) results in DNA stretching ~70% beyond its initial length without the need for any additional force [38,40,41]. Many studies have since investigated the intricacies of this change in DNA structure that in turn allows for such a dramatic shift in DNA elasticity [42,43].

Rotary motors: flagella

Bacteria including *E. Coli* swim using single or multiple flagella that are driven by a reversible rotary motor at its base. This molecular motor is ~45 nm in diameter and powered by an ion gradient. The torque generated by the rotary motor is transferred to a helical filament via a hook (~80 nm long) causing the filament to rotate in a propeller like fashion. Optical tweezers have proven useful in measuring torque generated by flagella rotation in addition to characterising the biomechanics of motion. In seminal works by Block et al. the bacteria are tethered to a fixed surface with external torque applied by the trapping laser using beam steering optics [44]. This showed that bacterial flagella act as linear torsion springs for half of a full rotation, beyond this the flagella became more rigid. Subsequently, Berry et al. used a similar set-up with the exception that a trapped particle was used to stall the flagella. This facilitated measurement of the generated torque (~4500 pN nm), which occurred at all angles of the flagella irrespective of whether it was stalled, or allowed to progress forwards or driven backwards [45]. This study also showed that these motors are capable of backwards rotation and thus not connected to ion transport where transport in the opposite direction is dramatically limited. This provides important insights as to how these motors function.

Others have characterised the force of flagella by optically trapping single bacteria in a microfluidic chamber and combined this with imaging (e.g. fluorescence) [46,47]. In this case the barrel-shaped motile bacteria are held between two optical traps with monitoring of flagella

position performed using both optical traps and by imaging the light from each of the tweezers beams onto two photodetectors. Using this approach, bacterial flagella were shown to exert two types of rotation: rotation of the flagella and subsequent rotation of the barrel shaped body. The resultant motion was either progressive in nature or tumbling. Further advancements in imaging have enabled researchers to monitor multiple flagella simultaneously to determine the mechanics of rotation [46].

6 Cells

Optical tweezers have also seen use in numerous cellular assays. We describe some of the key studies enabled by optical tweezers. At the cell scale, they range from cell patterning and organisation to microrheology and controlled studies of cell migration and fusion. Several cell types have been studied including primary human cells, embryonic stem cells, bacteria and red blood cells. Optical tweezers have featured in hemorheological studies including the dynamics and biophysics of leukocytes and platelets [48].

6.1 Cell patterning

In biology, topology is a key factor in cell lineage selection and development. To study this effect, positioning and organising cells in arbitrary geometries would be advantageous. In particular, embryonic stem cells are of major interest for such studies. With optical tweezers direct organisation and manipulation of embryonic stem cells at a precise level was demonstrated (Figure 4a-c) [49]. Alternatively, direct optical trapping for organisation has also used a photonic-crystal platform. This has enabled trapping and cell organisation with low power requirements and improved force efficiency. Jing et al used such a system for mammalian fibroblast, yeast, and *E. coli* cells. This technology inherits the versatility from conventional optical tweezers and improves trapping-force efficiency by using a photonic-crystal substrate, without compromising cell viability [49].

Multiplexed traps can enable widespread patterning of living cells. A study in 2006 showed heterotypic networks of living cells in hydrogel. The team showed cell positioning at submicron precision with an intercell separation <400 nm, which enabled generation of a network of mouse fibroblasts surrounded by a ring of bacteria. Separately hundreds of *Pseudomonas aeruginosa* were positioned in two and three dimensional arrays. There is promise in using such organisation for more detailed studies of cell differentiation and tissue development (Figure 4d-f) [50].

[Figure 4 near here]

6.2 Microrheology

The response in terms of deformation and flow of biological material subjected to an applied force may give researchers insight into the complex mechanical properties of cells and tissue. Many show viscoelasticity: the response to strain exhibits neither liquid-like viscosity or solid-like elasticity, rather a combination of the two. Bulk rheology studies have prevailed where strain is applied to the whole sample and the bulk stress response is recorded. The drawback is that operating at such scales does not extract information relating to heterogeneities or size-dependent aspects of the sample response.

As a result, methods for microrheology have emerged to determine viscoelasticity within microlitre volumes. Passive microrheology approaches track microspheres embedded in the material that are freely diffusing, to determine both the frequency-dependent elastic modulus and viscous modulus. The Stokes–Einstein relations may be used to relate the microparticle trajectories to viscoelastic properties. In contrast to the passive approach, we may move a microparticle through the material and perform active microrheology. This widens the applicability and parameter space of study. Optical tweezers are excellent for active microrheology, measuring miniscule forces with high precision (spatio-temporal, nanometre

and millisecond) [51]. A variant of optical tweezers based microrheology with traps can be performed with rotating rather than translating microparticles. Notable studies in this area with optical traps has included synthetic polymers, DNA, actin, microtubules, intermediate filaments, moving up to viscous fluids including mucus and vitreous humor.

By reconsidering the physics of the counter-propagating dual beam trap, Guck et al. showed a new insight into the behaviour of deformable objects placed in such a system. The momentum of light is proportional to the refractive index n of the medium within which the light is travelling, according to the Minkowski formulation. This means when light passes from the sample medium to the cell (and back out again) a momentum change occurs at the interface that results in a force *away* from the medium of higher refractive index. For a deformable object such as a cell held in a counter-propagating trap system, this counter-intuitive outcome means the cell bulges outwards from the light beams [52]. The deformation of the cell is also indicative of the mechanical properties of the cell which can vary from normal to neoplastic conditions. Guck et al used this *cell stretcher* (Figure 5a-b) to explore a range of cancer and blood cells where the very deformation of the cell within the counter-propagating beam trap was correlated with the degree of neoplasia (cancer). This label-free mechanical phenotyping approach has been applied to breast and oral cancer with encouraging results [53,54].

Turning to traditional optical tweezers, they have enabled viscoelastic measures of cell deformation through tether formation. A powerful approach has been utilising polymer microbeads to act as handles, each attached to opposing ends of cells. In this way, a cell stretching assay can be achieved in a geometry [55] that complements the counter-propagating dual beam cell stretcher developed by Guck et al [53]. Optical tweezers have enabled investigation of many aspects of red blood cell mechanics and function including elasticity, shape and electrochemical charge in addition to alterations due to disease state (reviewed in [56]). As an example, Mills et al used Stokes' law of force deformation in fluid viscosity to

measure extraction forces using trapped microbead handles directly attached to one or opposing ends of red blood cells (Figure 5c-d), in a geometry akin in appearance to the actin-dumbbell (Figure 2c) [57]. By indirectly or directly trapping erythrocytes and measuring tensile forces, recent work has been able to define elasticity changes of erythrocytes following drug treatment or pathology onset [58,59]. Though predominantly used in erythrocytes, tether formation has been employed to measure viscoelastic changes related to cell differentiation. In studies of human and mouse stem cells, optical tweezers demonstrate changes in cell membrane tension associated with differentiation state [60-62].

[Figure 5 near here]

6.3 Guiding cell growth

Determining what cues and factors cause directional cell growth may enable researchers to understand underlying mechanisms of cell repair, cell migration, and establishment of cell connection. Here we show examples where optical tweezers have directed such cell growth through either direct or indirect means.

By directly focusing a laser beam at the leading edges of developing growth cones of a neuronal cell, Ehrlicher and colleagues observed that lamellipodia extension could be directed towards a particular direction [63] (Figure 6a). This effect was attributed to how the optical gradient force of the focused beam attracts actin monomers at that particular edge. This creates a pool of monomers that are required for actin-polymerization events key to lamellipodia growth [64]. Further studies showed filopodia alignment to an applied optical field may direct growth [65].

Beyond direct induction of monomers, optical tweezers may be used to initiate chemotaxis for directed cell growth. Chemotaxis refers to the migration of cells toward attractant chemicals or away from repellents. Virtually all motile organisms show some form

of chemotaxis. The chemotactic responses of eukaryotic cells involve regulation of cytoskeletal elements (actin or microtubule). Optical tweezers can move engineered, micron-sized particles containing a molecular cargo to any point in a sample for controlled release [66]. This enables characterisation of a cell's response to such stimuli from various positions. Kress et al explored the motility of single human leukaemia cells in this way and showed directed migration towards the chemoattractant formyl-methionine-leucine-phenylalanine (Figure 6b), and repulsion from released cytochalasin D, an inhibitor of actin polymerisation (necessary for cell extension and motility).

Alternatively, rather than directly using optical forces, or tweezing such engineered particles to release molecules, traps can create specific flows and forces adjacent to cells. This can have a major impact: as an example, a rotating trapped particle held adjacent to the axonal projection of a nerve cell guided the cell's extension. The physics of how we set such particles into rotation is described in section 8. In this case, the particle rotation created a localised microfluidic flow in turn resulting in a sub pN shear force against the growth cone. The cone in turn responds to this shear (Figure 6c). This light driven micromotor demonstrated that the axonal direction and growth could be influenced in this novel manner [67]. All these examples are seen in Figure 6 and demonstrate some of the routes researchers have explored using traps for cell growth.

[Figure 6 near here]

6.4 Cell fusion

Whilst we have concentrated on laser light exerting a force, laser light may also cut or surgically remove material. The details of this depend upon parameters such as the laser wavelength and whether it is running in pulsed or continuous wave mode. Only a few years after their development, optical tweezers were combined with a pulsed UV laser microbeam to

demonstrate laser microsurgery leading to cell fusion, in this case without invoking chemical or electrical methods. This enabled a step change in the manner biologists considered the generation of viable hybrid cells [68]. Chen et al used this approach, successfully fusing embryonic stem cells with somatic cells. Such studies may lead to a better understanding of cell differentiation and reprogramming [69]. A more detailed discussion of this topic may be found elsewhere [70].

7 Optical Manipulation at large scales and *in vivo*

The dual beam counter-propagating geometry has found rich applications including as a cell stretcher, and trapping with other analytical modes (e.g. fluorescence or Raman detection). Studies have consistently shown it is highly favourable in trapping larger objects and can obviate laser damage issues due to its use of divergent, gently focused light beams. In particular, the absence of high numerical aperture optics, large capture range and fibre implementation mean it is compatible with higher throughput and microfluidic geometries when compared to three dimensional optical tweezers. Beyond *in vitro* manipulation, optical forces have also been explored as an instrument for *in vivo* manipulation and trapping assays. This counter-propagating geometry has been invigorated in the last decade due to new embodiments and applications. An example is 'macro-tweezers'. In this study a spatial light modulator (SLM, see later) shaped the standard Gaussian beam into two beams each with a different divergence [71]. These were imaged into the probe chamber, creating two axially separated focal spots. After reflection of one of the beams at the mirror behind the sample, a light configuration – the “macro-tweezers”, similar to a counter-propagating fibre trap, was realised. Three-dimensional all-optical trapping and guiding was achieved in a volume of around 4 mm³. The work focused upon studies of actively swimming organisms, for example *Euglena* protists and dinoflagellates of up to 70 µm length. The lower power density reduced photodamage and heating issues [71].

Trapping in zebrafish, a now popular assay, obviated the need for the light field to penetrate opaque external barriers which would be the case for other organisms. This ability to manipulate exogenous particles within zebrafish with optical tweezers was reported in 2016. In that study, by injecting cell adherent nanoparticles of high refractive index, Johansen et al were able to use multiplexed optical tweezers to trap and measure deformability of internal endothelial cells, erythrocytes and macrophages [72].

Structures however need not be adhered to exogenous nanoparticles for manipulation at the *in vivo* scale. In a study by Favre-Bulle et al, optical tweezers were used to trap otoliths within zebrafish (Figure 7). These are ear stones which may produce fictive vestibular stimuli in zebrafish [73]. The otoliths were around 55 microns in diameter providing a major challenge for optical manipulation. The study calculated the optical force using the ray optics method whilst accounting for light scattering characteristics of biological tissues, refractive index. This included using a light deflection method for recording and accounting for the spatial variation in the refractive index across each otolith: This influences the locations and directions of the optical forces. The study was able to identify the corrective tail movements that accompany otolith stimulation, a mechanism produced by zebrafish to correct their spatial positioning. Although the significance in direct trapping provides a novel potential for *in vivo* targeting, accurate beam positioning is required, with beam drifts of $<2 \mu\text{m}$ away from optimal position inducing a significant drop in optical force ($\sim 20\%$). These reports show new directions for trapping and understanding *in vivo* nanoparticle-cell interaction in drug treatment or cell-cell interaction in a whole organism. Moving onto higher order organisms, *in vivo* trapping of erythrocytes within subdermal blood capillaries of a mouse ear has also been reported [72]. The capillary depth matched the working distance for tweezers making this study feasible. In the same study the authors used tweezers to clear a blocked microvessel. It is to be noted that

standard optical tweezers are restricted to tissues that are highly vascularised, with these vessels close to the surface of the skin. More advanced *in vivo* studies in future would benefit from aberration correction to implement trapping at depth [74,75].

[Figure 7 near here]

8 Laser Heating and Damage

So far, we have considered how light may exert a force on a range of mesoscopic particles including cells. Whether contact with light is direct or indirect, for all forms of optical manipulation we also need to consider the absorption, heating and subsequent potential damage that might accrue due to the application of laser light. This is particularly pertinent for sensitive molecules and cells and can be a major issue in optical tweezers where we tightly focus light. From a biological perspective there are a range of approaches to identify cell damage. The short-term (immediate) impact, cellular uptake of propidium iodide for example indicates rupture of cell membranes which can result in cell death. Longer-term damage is more challenging to measure: quantification of cell cloning efficiency as well as screening for cell anomalies in derivative populations may be effective studies in this regard [76].

Ashkin's first studies showed that cellular light exposure assays that aim to maintain biological integrity typically favoured longer wavelength light (NIR) for trapping [77]. In the visible or ultraviolet region of the spectrum biological integrity may be compromised with deleterious photochemical reactions and reactive oxygen species generation [78,79]. Further studies in the literature have demonstrated that even working in the NIR may still cause significant impact to cellular health. This may include in reduced clonal growth, decline in bacterial motility, and cell death [80].

Practically today, optical tweezers typically operate with laser wavelengths in the near infra-red region of the spectrum (the so-termed therapeutic window for biological studies extends from around 650 nm-1350 nm) to minimise damage and heating. It is important to note that such damage and heating may take place within the liquid medium, within an inert trapped particle or the biological specimen itself. A rigorous evaluation of these effects is key to understanding how optical tweezers can be most effective. Optical tweezers use modest laser power but as the light is tightly focused power densities may reach \sim MW/cm². In 2002, Peterman and Schmidt developed a trapping model that incorporated heat generation due to optical absorption around a focused beam at 1064 nm. In this model they considered the outward heat flow, and heat sinking by the glass surfaces of the sample chamber [81]. They saw that in the most common scenarios (for studies using micron-sized polystyrene or silica beads), absorption of the laser light in the liquid bath around the trapped particle, not in the particle itself, was the key contribution to heating. Experiments recorded the spectrum of the Brownian motion of trapped beads in water and in glycerol as a function of the trapping laser intensity to verify the predictions. Interestingly, heating of the medium thus has a non-negligible effect on trap calibration in typical biophysical experimental circumstances. This should be taken into consideration particularly when higher laser powers (>100 mW) are used. From a physics standpoint heating within the liquid or the trapped particle can be an issue that may deflect from the accuracy of measurement. In addition to local temperature changes, such heating would alter the local viscosity surrounding the particle. Other studies have explored the heating due to translation and rotation.

Laser damage and heating considerations are not solely for single beam optical tweezers. Near field traps (see section 8.2) often use surface plasmons for enhancing optical forces. These are coherent electron oscillations moving in unison with an electromagnetic wave along the interface between a dielectric and a metal. These dissipate and lead to thermal effects

that have to be considered along with optical forces. The dual beam counter-propagating trap which we have described for cell stretching may be used to study thermal effects upon cells. A study used the spreading of cells as a novel, sensitive viability marker. The optical stretcher was used to simulate heat shocks that cells typically experience during measurements in manipulation studies. The results showed that about 60% of the cells survived the heat shocks without critical damage at temperatures of up to 58°C [82]. It is important to note the mechanical properties of a cell may change with temperature. The optical stretcher incorporated a separate laser operating at a wavelength of 1480 nm solely for heating. This allowed a study of the degree of thermal softening of cells in the passive viscoelastic regime, and observing cell contraction whenever the overall temperature exceeded 52°C [83]. Overall, these studies show optical forces normally go hand-in-hand with potential damage or thermal effects. From a biological perspective a careful examination of these is essential for any new study to ensure the validity of the data.

9 Advanced topics in optical manipulation

9.1 Structured light

The advent of optical beam shaping both in phase, amplitude and polarisation with an array of technology has enabled this area in recent years. Multiplexing traps has been essential to perform biological studies. Indeed, for single molecule studies we often require two or three traps which are typically generated using acousto-optic deflectors or multiple paths in the beam geometry. These approaches are largely restricted to two dimensions. To achieve full three dimensional control of each individual trap, we may use holographic optical tweezers [84]. These may be implemented using liquid crystal devices such as a spatial light modulator (SLM) that can allow full control over the phase and amplitude of light. In turn this can allow researchers to create multiple traps in a three-dimensional space. Furthermore, the versatility

of SLMs means we can shape the light to compensate for aberrations as well as create more advanced forms of propagating light fields, so termed structured light [5]. This generally refers to a range of transverse mode profiles, moving away from a standard zeroth order Gaussian beam. This includes vectorial fields where the polarisation of the field plays an integral role. In the last three decades, light fields possessing angular momentum (spin and orbital) have enabled trapping studies where transfer of optical angular momentum from the beam to the trapped particle causes rotation (see later). Propagation invariant beams have shown extended transport of particles and motion of particles and cells on more complex trajectories. Structured light creates extended optical patterns in both two and three dimensions that may be termed potential energy landscapes. Particle and cell motion across such landscapes is intricately linked to the physical response of the cell to the underlying optical field resulting in a differential motion – sorting. A major body of work has looked at the use of optical forces to separate or fractionate particles, notably cells. The motion of particles over such potential energy landscapes has been a rich playground for physics-based studies. It is reasonable to say the prospect for their use for cell separation may be hampered by throughput and selectivity though work has shown success on some cell types notably erythrocytes and leukocytes. Traps can also be used to select particles from flow cytometer type geometries. We refer the reader elsewhere for a review of this topic and its broader implications [85].

Even reverting back to a single beam trap, the role of the polarisation state of the trapping beam can play a profound role. As a prime example, circularly polarised light is known to possess spin angular momentum of value $\pm\hbar$ per photon. Intriguingly by trapping birefringent particles one can set these into rotation due to the trapped object acting as a waveplate and a torque being exerted due to the passage of light through the object [86]. This is not the only route to implement rotation of trapped objects and we refer the reader to a comprehensive recent paper that describes rotational dynamics in more depth [87]. The original

work on rotating particles was performed with calcite particles. However, a large subsequent effort developed birefringent particles of known size and shape for trapping purposes. A suite of anisotropic colloids have emerged for such use including the microsphere vaterite [88]. Such crystals have been used for rotation. Upon trapping, these particles reach a terminal angular velocity due to a balance between the optical torque applied from the trapping beam and the rotational Stokes drag from the liquid environment [89,90]. From the biology perspective, we have already described the use of such rotating particles for directed cell growth. At the molecular scale, an example of a key experiment using such spinning particles was the observation of RNA polymerase translocation in real time as it worked under a defined torque. In this experiment, RNA polymerase was torsionally anchored to a coverslip. The end of the DNA template was torsionally anchored to the bottom of a nanofabricated quartz cylinder held in an angular optical trap. This study revealed that RNA polymerase adapts its biomechanical behaviour when encountering a region of supercoiled (over- or underwound) DNA. In these conditions, RNA polymerase slows and pauses more frequently than previously observed. It is also able to produce sufficient torque (11 ± 4 pN.nm) to alter DNA structure which allows transcription to continue [91]. For rotating particles, studies showed spinning vaterite may be used as a microviscometer for human tear fluid, recording a viscosity value of 1.1 ± 0.1 cP. In the absence of a tear response, between 1 μ l and 5 μ l of eye fluid can be collected. This shows the importance of such a study for fluids where biological samples are precious and hard to obtain [92].

9.2. Optical trapping in the near field

The optical manipulation methods we have discussed so far all use free space optics and as such we are constrained to free space Gaussian beam propagation. Interestingly, there has been a huge impetus in the last two decades to move to the near field in a variety of ways. Importantly the near field can circumvent the so termed diffraction limit making it possible to create

features of the optical field. In contrast to propagating fields, evanescent fields can be focused beyond the diffraction limit, making it possible to create strong optical field gradients in excess of those that can be achieved in far field, thus yielding stronger forces, as the gradient force is proportional to ∇I . Evanescent fields may be generated by plasmonic nanostructures or dielectric waveguides and can be enhanced using cavity approaches [93-95]. Moreover, compared to the three-dimensional nature of optical tweezers working in the near field lends itself to a planar geometry so we may multiplex trap systems in a manner compatible for lab on chip or microfluidic applications. There are several drawbacks though to such systems, including ohmic heating in plasmonic traps, and difficulties in loading the trapping systems.

Interesting studies can be performed though with regard to very small biological samples. In contrast to the single molecule studies described above, nanofilm traps have demonstrated the *direct* optical trapping of a single bovine serum albumin (BSA) molecule that has a hydrodynamic radius of 3.4 nm, using a double-nanohole in an Au film. The strong optical force in the trap not only stably traps the protein molecule but also unfolds it. The unfolding of the BSA is confirmed by experiments with changing optical power and with changing solution pH [96]. It is important to remark that the absence of a strong gradient field and the relatively low polarizability of a single molecule would preclude such trapping in a standard optical tweezers system given how the forces relate to these parameters (see section 3). More broadly, nanoaperture optical tweezers are emerging as useful label-free devices for both the detection and identification of individual biological molecules and their interactions. Nanoaperture optical tweezers provide inexpensive and scalable method to observe real-time dynamics and to quantify binding kinetics of protein–small molecule interactions without the need to use tethers or labelling. Such nanoaperture-based optical tweezers have been used to trap and isolate single DNA molecules and to study proteins such as p53, a tumour suppressor gene that is frequently mutated in human cancers to render it either inactive or in fact promote

tumorigenesis. As we look forward, new trapping modes that use nanostructures, metasurfaces and other routes to create highly localised light fields will prove more important for biomedical research. There is ample scope here for materials science to contribute to new future trap geometries creating strong localised force fields [97].

10 Multimodality: combining optical traps with other techniques

Optical tweezers have been a *tour de force* in precision measurements in biomedicine. However, it has also found rich application for the life sciences when combined with other modalities such as laser microsurgery, which we have already described in relation to cells (section 6.4). A further area of application has been the combination of trapping with imaging modalities. This is perhaps not surprising given the response of biological systems to light-based excitation through processes such as autofluorescence, fluorescence with both endogenous and exogenous fluorophores and inelastic (Raman) scattering to recover molecular level information. Here we touch upon some combinations seen with tweezers and such imaging. Key technological advances in this area resides in choice of decoupling (or not) the trapping beam path with the imaging path and the mismatch of power densities required for imaging versus trapping. The presence of the trapping laser may cause deleterious photobleaching or in general just hamper faithful recording of the image.

In many studies of single molecules optical traps were combined with advanced (label-free) imaging methods. For example, optical tweezers with differential interference contrast microscopy (DIC) employed the same laser for trapping and displacement for the determination of the step size of kinesin [19]. The challenge of adding optical trapping with wide field epifluorescence microscopy resides in recording the fluorescence emission of a few fluorophores when we simultaneously have a relatively large optical trapping power, orders of magnitude higher in intensity. The system requires careful delineation between the trapping and

fluorescence emission light. This can be achieved using special multilayer thin-film optical filters and resorting to approaches such as cycling between the trapping and excitation beams [98]. Optical tweezers can furthermore be combined with standard fluorescence and imaging as well as multiphoton microscopy [99]. The imaging laser in this latter case—generating ultrashort pulses—may also be used to perform laser microsurgery, to perforate the membrane of trapped spermatozoa. Perforation of the cell membrane at the tail results in immobilisation of the sperm [100]. Immobilisation is required for clinical *in vitro* fertilisation (IVF) when a sperm is injected directly into the oocyte in a process known as intracytoplasmic fertilisation (ICSI). Laser microsurgery circumvents the use of chemicals to immobilise sperm, which can be toxic. Importantly, laser microsurgery induced immobilisation results in successful fertilisation of oocytes by ICSI and may be a clinically useful technique.

To date, experimental configurations have also employed combinations of the single beam optical tweezers trap and Raman spectroscopy using either the same beam or separate beams for Raman interrogation and trapping [101]. Using the same optics and microscope objective for trapping and Raman studies can add simplicity though reduces flexibility in geometry and potentially recording appropriate fields of view for the Raman image. A dual beam counter-propagating fibre trap may immobilise a cell and be combined with an orthogonally placed microscope objective to obtain molecular Raman spectra as seen in studies of large (30 μm diameter) trapped primary human keratinocyte cells. Subsequent imaging obtained Raman spectra from local parts of the trapped cell [102].

Optical imaging itself has undergone a revolution in the last two decades both attaining super-resolution, recognised in the 2014 Nobel Prize in Chemistry, and in recording wide field and depth information from larger samples in a rapid fashion. Essentially, at many relevant biological size scales we are keen to perform tomography of the sample. Optical tweezers have been added to imaging systems to create novel multimodal platforms. As an example, Huser et

al explored the use of holographic optical tweezers with (super-resolved) localisation microscopy. The trap allowed the bacterial cells to be turned and rotated. The team were able to explore nanoscale organisation of chromosomal DNA in the bacteria [103]. Turning to the counter-propagating trap geometry, Kreysing and colleagues developed the optical cell rotator (OCR) [104]. As with the Constable et al [9] study optical fibers delivered the light fields. However, in this instance one of the two trapping beams was asymmetric and used to rotate the sample. The rotation of cells around an axis perpendicular to the optical axis of the microscope, and as with the Jess et al study, the system was decoupled from the optical detection path. The results showed data on human erythrocytes, promyelocytic leukaemia cells, and cell clusters. This forms a new method for tomographic microscopy [104].

At the larger size scale, we have seen the emergence of an imaging approach employing a sheet of light to illuminate a sample, where the fluorescent imaging path is perpendicular to the illuminated plane. This geometry termed light sheet imaging (or selective plane microscopy) offers key advantages including rapid acquisition of images and low photodamage. Optical tweezers have been used in tandem with light sheet imaging to exert local forces and develop a predictive mechanical model of cell contact within the early *Drosophila* embryo. Counter-propagating dual beam optical traps may provide new forms of sample manipulation for light sheet studies but the forces may be too weak to hold larger organisms [105]. It is not only light waves that can manipulate particles: sound waves may exert a force as well and the strength of this interaction mean it is better suited to holding larger specimens [106] including samples such as embryos for analysis in light sheet imaging [107]. Combining both optical and acoustic forces is also very worthy of consideration and can yield the ‘best of both worlds’ in terms of range of force and precision, to achieve new levels of control over micro-organism motion [108].

11 Conclusions

It is now over fifty years since Ashkin published his first work on the application of optical forces. This is a field that has grown in importance and retained centre stage for a plethora of biological studies that were simply not possible before the advent of optical manipulation. This review has given an insight into the biological relevance and importance of Ashkin's discoveries. Optical traps have emerged as a mainstay of biological science, operating on spatial and temporal scales of relevance.

It is a method that has crossed disciplines in a powerful and convincing way. The ingenuity lies in the method itself and its ability to discern quantifiable metrology on biological systems giving unprecedented insights. Its recent use *in vivo* represents a most exciting advancement where future discoveries will occur *in situ*: the most biologically relevant environment. In terms of single molecule assays, advancements may depend more on the discipline of biology. For example, how to adhere proteins without affecting function, as commonly occurs with protein linkages, or how to control molecular alignment. The next few decades will bring ever more detailed science to this area. We expect to see further advances particularly on novel tailored trapping geometries and incorporating traps with other methods, not necessarily just based in optics, for the biosciences.

Acknowledgements

This work was supported by the UK Engineering and Physical Sciences Research Council under Grant EP/P030017/1; The Hospital Research Foundation under Grant C-MCF-58-2019. CC thanks the University of Adelaide and University of Nottingham for the award of a PhD scholarship.

Disclosure statement

The authors have nothing to declare.

Notes on contributors



Carl Adrian Campugan is a PhD student jointly between the Faculty of Health and Medical Sciences at the University of Adelaide, Australia and the Faculty of Engineering at the University of Nottingham, UK. Carl's involvement in the subject article stems from his keen interest in the optical manipulation of biological cells. In particular, his PhD project aims to implement trapping techniques in to better understand early mammalian development.



Dr Kylie Dunning is a Hospital Research Foundation Fellow at the University of Adelaide, Australia. Kylie leads the Reproductive Success team within the Robinson Research Institute, where they use light-based technologies to better understand the biology that underpins successful development of the oocyte and early embryo. In 2020, in recognition of research excellence and community outreach, she was awarded The South Australian Tall Poppy of the Year Award, the HDA Women's Excellence in Research Award and the Robinson Research Institute Director's Award.



Kishan Dholakia is Professor at the University of St Andrews, Scotland. He works on advanced optical beam shaping for biophotonics, precision measurement and optical manipulation. He is a fellow of the Royal Society of Edinburgh, the Optical Society, SPIE and the Institute of Physics (IOP). He is recipient of the R.W. Wood Prize of the Optical Society (2016), the Institute of Physics Thomas Young Medal and Prize (2017) and the SPIE Dennis Gabor Award (2018).

References

1. Nichols EF, Hull GF. A preliminary communication on the pressure of heat and light radiation. *Physical Review (Series I)*. 1901;13(5):307.
2. Nichols EF, Hull GF. The pressure due to radiation.(second paper.). *Physical Review (Series I)*. 1903;17(1):26.
3. Lebedev P. Experimental examination of light pressure. *Nuovo Cimento*. 1883;15(195):195.
4. Perkins TT. Optical traps for single molecule biophysics: a primer. *Laser & Photonics Reviews*. 2009;3(1-2):203-220.
5. Dholakia K, Čižmár T. Shaping the future of manipulation. *Nature Photonics*. 2011;5(6):335-342.
6. Jones PH, Maragò OM, Volpe G. *Optical tweezers: Principles and applications*. Cambridge University Press; 2015.
7. Millen J, Stickler BA. Quantum experiments with microscale particles. *Contemporary Physics*. 2020:1-14.
8. Ashkin A. Acceleration and trapping of particles by radiation pressure. *Physical Review Letters*. 1970;24(4):156.
9. Constable A, Kim J, Mervis J, et al. Demonstration of a fiber-optical light-force trap. *Optics Letters*. 1993;18(21):1867-1869.
10. Ashkin A, Dziedzic JM, Bjorkholm JE, et al. Observation of a single-beam gradient force optical trap for dielectric particles. *Optics Letters*. 1986;11(5):288-290.
11. Montange RK, Bull MS, Shanblatt ER, et al. Optimizing bead size reduces errors in force measurements in optical traps. *Optics Express*. 2013;21(1):39-48.
12. Novotny L, Hecht B. *Principles of nano-optics*. Cambridge university press; 2012.

13. Roichman Y, Sun B, Stolarski A, et al. Influence of nonconservative optical forces on the dynamics of optically trapped colloidal spheres: the fountain of probability. *Physical Review Letters*. 2008;101(12):128301.
14. Greenleaf WJ, Woodside MT, Abbondanzieri EA, et al. Passive all-optical force clamp for high-resolution laser trapping. *Physical Review Letters*. 2005;95(20):208102.
15. Farré A, Marsà F, Montes-Usategui M. Optimized back-focal-plane interferometry directly measures forces of optically trapped particles. *Optics Express*. 2012;20(11):12270-12291.
16. Thalhammer G, Obmascher L, Ritsch-Marte M. Direct measurement of axial optical forces. *Optics Express*. 2015;23(5):6112-6129.
17. Strasser F, Moser S, Ritsch-Marte M, et al. Direct measurement of individual optical forces in ensembles of trapped particles. *Optica*. 2021;8(1):79-87.
18. García LP, Pérez JD, Volpe G, et al. High-performance reconstruction of microscopic force fields from Brownian trajectories. *Nature Communications*. 2018;9(1):1-9.
19. Svoboda K, Schmidt CF, Schnapp BJ, et al. Direct observation of kinesin stepping by optical trapping interferometry. *Nature*. 1993;365(6448):721-727.
20. Kojima H, Muto E, Higuchi H, et al. Mechanics of single kinesin molecules measured by optical trapping nanometry. *Biophysical Journal*. 1997 Oct;73(4):2012-22.
21. Visscher K, Schnitzer MJ, Block SM. Single kinesin molecules studied with a molecular force clamp. *Nature*. 1999;400(6740):184-189.
22. Schroeder III HW, Hendricks AG, Ikeda K, et al. Force-dependent detachment of kinesin-2 biases track switching at cytoskeletal filament intersections. *Biophysical Journal*. 2012;103(1):48-58.
23. Gennerich A, Carter AP, Reck-Peterson SL, et al. Force-induced bidirectional stepping of cytoplasmic dynein. *Cell*. 2007;131(5):952-965.

24. Reck-Peterson SL, Yildiz A, Carter AP, et al. Single-molecule analysis of dynein processivity and stepping behavior. *Cell*. 2006;126(2):335-348.
25. Coppin CM, Pierce DW, Hsu L, et al. The load dependence of kinesin's mechanical cycle. *Proceedings of the National Academy of Sciences*. 1997;94(16):8539-8544.
26. Kojima H, Muto E, Higuchi H, et al. Mechanics of single kinesin molecules measured by optical trapping nanometry. *Biophysical journal*. 1997;73(4):2012-2022.
27. Hall K, Cole D, Yeh Y, et al. Kinesin force generation measured using a centrifuge microscope sperm-gliding motility assay. *Biophysical Journal*. 1996;71(6):3467-3476.
28. Fehr AN, Asbury CL, Block SM. Kinesin steps do not alternate in size. *Biophysical Journal*. 2008;94(3):L20-L22.
29. Nicholas MP, Berger F, Rao L, et al. Cytoplasmic dynein regulates its attachment to microtubules via nucleotide state-switched mechanosensing at multiple AAA domains. *Proceedings of the National Academy of Sciences*. 2015;112(20):6371-6376.
30. Mallik R, Carter BC, Lex SA, et al. Cytoplasmic dynein functions as a gear in response to load. *Nature*. 2004;427(6975):649-652.
31. Finer JT, Simmons RM, Spudich JA. Single myosin molecule mechanics: piconewton forces and nanometre steps. *Nature*. 1994;368(6467):113-119.
32. Sakamoto T, Amitani I, Yokota E, et al. Direct observation of processive movement by individual myosin V molecules. *Biochemical and biophysical research communications*. 2000;272(2):586-590.
33. Molloy J, Burns J, Kendrick-Jones J, et al. Movement and force produced by a single myosin head. *Nature*. 1995;378(6553):209-212.
34. Wang MD, Schnitzer MJ, Yin H, et al. Force and velocity measured for single molecules of RNA polymerase. *Science*. 1998;282(5390):902-907.

35. Shaevitz JW, Abbondanzieri EA, Landick R, et al. Backtracking by single RNA polymerase molecules observed at near-base-pair resolution. *Nature*. 2003;426(6967):684-687.
36. Gabizon R, Lee A, Vahedian-Movahed H, et al. Pause sequences facilitate entry into long-lived paused states by reducing RNA polymerase transcription rates. *Nature Communications*. 2018;9(1):1-10.
37. Abbondanzieri EA, Greenleaf WJ, Shaevitz JW, et al. Direct observation of base-pair stepping by RNA polymerase. *Nature*. 2005;438(7067):460-465.
38. Smith SB, Cui Y, Bustamante C. Overstretching B-DNA: the elastic response of individual double-stranded and single-stranded DNA molecules. *Science*. 1996;271(5250):795-799.
39. Wang MD, Yin H, Landick R, et al. Stretching DNA with optical tweezers. *Biophysical Journal*. 1997;72(3):1335-1346.
40. Cluzel P, Lebrun A, Heller C, et al. DNA: an extensible molecule. *Science*. 1996;271(5250):792-794.
41. Schakenraad K, Biebricher AS, Sebregts M, et al. Hyperstretching DNA. *Nature Communications*. 2017;8(1):1-7.
42. King GA, Gross P, Bockelmann U, et al. Revealing the competition between peeled ssDNA, melting bubbles, and S-DNA during DNA overstretching using fluorescence microscopy. *Proceedings of the National Academy of Sciences*. 2013;110(10):3859-3864.
43. van Mameren J, Gross P, Farge G, et al. Unraveling the structure of DNA during overstretching by using multicolor, single-molecule fluorescence imaging. *Proceedings of the National Academy of Sciences*. 2009;106(43):18231-18236.

44. Block SM, Blair DF, Berg HC. Compliance of bacterial flagella measured with optical tweezers. *Nature*. 1989;338(6215):514-518.
45. Berry RM, Berg HC. Absence of a barrier to backwards rotation of the bacterial flagellar motor demonstrated with optical tweezers. *Proceedings of the National Academy of Sciences*. 1997;94(26):14433-14437.
46. Mears PJ, Koirala S, Rao CV, et al. *Escherichia coli* swimming is robust against variations in flagellar number. *Elife*. 2014;3:e01916.
47. Min TL, Mears PJ, Chubiz LM, et al. High-resolution, long-term characterization of bacterial motility using optical tweezers. *Nature Methods*. 2009;6(11):831-835.
48. Avsievich T, Zhu R, Popov A, et al. The advancement of blood cell research by optical tweezers. *Reviews in Physics*. 2020;5:100043.
49. Jing P, Liu Y, Keeler EG, et al. Optical tweezers system for live stem cell organization at the single-cell level. *Biomedical Optics Express*. 2018;9(2):771-779.
50. Akselrod G, Timp W, Mirsaidov U, et al. Laser-guided assembly of heterotypic three-dimensional living cell microarrays. *Biophysical Journal*. 2006;91(9):3465-3473.
51. Robertson-Anderson RM. Optical Tweezers Microrheology: From the Basics to Advanced Techniques and Applications. *ACS Macro Letters*. 2018 2018/08/21;7(8):968-975.
52. Guck J, Ananthakrishnan R, Moon TJ, et al. Optical deformability of soft biological dielectrics. *Physical Review Letters*. 2000 Jun 5;84(23):5451-4.
53. Guck J, Schinkinger S, Lincoln B, et al. Optical deformability as an inherent cell marker for testing malignant transformation and metastatic competence. *Biophysical Journal*. 2005;88(5):3689-3698.
54. Remmerbach TW, Wottawah F, Dietrich J, et al. Oral cancer diagnosis by mechanical phenotyping. *Cancer Research*. 2009 Mar 1;69(5):1728-32.

55. Dao M, Lim CT, Suresh S. Mechanics of the human red blood cell deformed by optical tweezers. *Journal of the Mechanics and Physics of Solids*. 2003;51(11-12):2259-2280.
56. Zhu R, Avsievich T, Popov A, et al. Optical Tweezers in Studies of Red Blood Cells. *Cells*. 2020 Feb 26;9(3).
57. Mills J, Qie L, Dao M, et al. Nonlinear elastic and viscoelastic deformation of the human red blood cell with optical tweezers. *Molecular & Cellular Biomechanics*. 2004;1(3):169.
58. Sheikh-Hasani V, Babaei M, Azadbakht A, et al. Atorvastatin treatment softens human red blood cells: an optical tweezers study. *Biomedical Optics Express*. 2018;9(3):1256-1261.
59. Agrawal R, Smart T, Nobre-Cardoso J, et al. Assessment of red blood cell deformability in type 2 diabetes mellitus and diabetic retinopathy by dual optical tweezers stretching technique. *Scientific Reports*. 2016;6(1):1-12.
60. De Belly H, Stubb A, Yanagida A, et al. Membrane Tension Gates ERK-Mediated Regulation of Pluripotent Cell Fate. *Cell Stem Cell*. 2021 Feb 4;28(2):273-284 e6.
61. Titushkin I, Cho M. Distinct membrane mechanical properties of human mesenchymal stem cells determined using laser optical tweezers. *Biophysical Journal*. 2006;90(7):2582-2591.
62. Tan Y, Kong C-w, Chen S, et al. Probing the mechanobiological properties of human embryonic stem cells in cardiac differentiation by optical tweezers. *Journal of Biomechanics*. 2012;45(1):123-128.
63. Ehrlicher A, Betz T, Stuhrmann B, et al. Guiding neuronal growth with light. *Proceedings of the National Academy of Sciences*. 2002;99(25):16024-16028.
64. Dent EW, Gertler FB. Cytoskeletal dynamics and transport in growth cone motility and axon guidance. *Neuron*. 2003;40(2):209-227.

65. Carnegie DJ, Stevenson DJ, Mazilu M, et al. Guided neuronal growth using optical line traps. *Optics Express*. 2008 Jul 7;16(14):10507-17.
66. Kress H, Park J-G, Mejean CO, et al. Cell stimulation with optically manipulated microspheres. *Nature Methods*. 2009;6(12):905-909.
67. Wu T, Nieminen TA, Mohanty S, et al. A photon-driven micromotor can direct nerve fibre growth. *Nature Photonics*. 2012;6(1):62-67.
68. Steubing RW, Cheng S, Wright WH, et al. Laser induced cell fusion in combination with optical tweezers: the laser cell fusion trap. *Cytometry: The Journal of the International Society for Analytical Cytology*. 1991;12(6):505-510.
69. Chen S, Cheng J, Kong C-W, et al. Laser-induced fusion of human embryonic stem cells with optical tweezers. *Applied Physics Letters*. 2013;103(3):033701.
70. Blázquez-Castro A, Fernández-Piqueras J, Santos J. Genetic Material Manipulation and Modification by Optical Trapping and Nanosurgery-A Perspective. *Frontiers in Bioengineering and Biotechnology*. 2020;8:1118.
71. Thalhammer G, Steiger R, Bernet S, et al. Optical macro-tweezers: trapping of highly motile micro-organisms. *Journal of Optics*. 2011;13(4):044024.
72. Johansen PL, Fenaroli F, Evensen L, et al. Optical micromanipulation of nanoparticles and cells inside living zebrafish. *Nature Communications*. 2016;7(1):1-8.
73. Favre-Bulle IA, Stilgoe AB, Rubinsztein-Dunlop H, et al. Optical trapping of otoliths drives vestibular behaviours in larval zebrafish. *Nature Communications*. 2017;8(1):1-7.
74. Zhong M-C, Wei X-B, Zhou J-H, et al. Trapping red blood cells in living animals using optical tweezers. *Nature Communications*. 2013;4(1):1-7.
75. Čižmár T, Mazilu M, Dholakia K. In situ wavefront correction and its application to micromanipulation. *Nature Photonics*. 2010;4(6):388-394.

76. Liang H, Vu KT, Krishnan P, et al. Wavelength dependence of cell cloning efficiency after optical trapping. *Biophysical Journal*. 1996;70(3):1529-1533.
77. Ashkin A, Dziedzic JM, Yamane T. Optical trapping and manipulation of single cells using infrared laser beams. *Nature*. 1987;330(6150):769-771.
78. Kvam E, Tyrrell RM. Induction of oxidative DNA base damage in human skin cells by UV and near visible radiation. *Carcinogenesis*. 1997;18(12):2379-2384.
79. Liebel F, Kaur S, Ruvolo E, et al. Irradiation of skin with visible light induces reactive oxygen species and matrix-degrading enzymes. *Journal of Investigative Dermatology*. 2012;132(7):1901-1907.
80. Neuman KC, Chadd EH, Liou GF, et al. Characterization of photodamage to *Escherichia coli* in optical traps. *Biophysical Journal*. 1999;77(5):2856-2863.
81. Peterman EJ, Gittes F, Schmidt CF. Laser-induced heating in optical traps. *Biophysical Journal*. 2003;84(2):1308-1316.
82. Wetzel F, Rönicke S, Müller K, et al. Single cell viability and impact of heating by laser absorption. *European Biophysics Journal*. 2011;40(9):1109-1114.
83. Chan C, Whyte G, Boyde L, et al. Impact of heating on passive and active biomechanics of suspended cells. *Interface Focus*. 2014;4(2):20130069.
84. Curtis JE, Koss BA, Grier DG. Dynamic holographic optical tweezers. *Optics Communications*. 2002;207(1-6):169-175.
85. Dholakia K, MacDonald MP, Zemánek P, et al. Cellular and colloidal separation using optical forces. *Methods in Cell Biology*. 2007;82:467-495.
86. Friese ME, Nieminen TA, Heckenberg NR, et al. Optical alignment and spinning of laser-trapped microscopic particles. *Nature*. 1998;394(6691):348-350.

87. Bruce GD, Rodríguez-Sevilla P, Dholakia K. Initiating revolutions for optical manipulation: the origins and applications of rotational dynamics of trapped particles. *Advances in Physics: X*. 2021;6(1):1838322.
88. Fernández-Nieves A, Cristobal G, Garcés-Chávez V, et al. Optically anisotropic colloids of controllable shape. *Advanced Materials*. 2005;17(6):680-684.
89. Bennett JS, Gibson LJ, Kelly RM, et al. Spatially-resolved rotational microrheology with an optically-trapped sphere. *Scientific Reports*. 2013;3(1):1-5.
90. Bishop AI, Nieminen TA, Heckenberg NR, et al. Optical microrheology using rotating laser-trapped particles. *Physical Review Letters*. 2004;92(19):198104.
91. Ma J, Bai L, Wang MD. Transcription under torsion. *Science*. 2013;340(6140):1580-1583.
92. Parkin SJ, Knöner G, Nieminen TA, et al. Picoliter viscometry using optically rotated particles. *Physical Review E*. 2007;76(4):041507.
93. Juan ML, Righini M, Quidant R. Plasmon nano-optical tweezers. *Nature Photonics*. 2011;5(6):349.
94. Kawata S, Sugiura T. Movement of micrometer-sized particles in the evanescent field of a laser beam. *Optics Letters*. 1992;17(11):772-774.
95. Reece PJ, Garcés-Chávez V, Dholakia K. Near-field optical micromanipulation with cavity enhanced evanescent waves. *Applied Physics Letters*. 2006;88(22):221116.
96. Pang Y, Gordon R. Optical trapping of a single protein. *Nano Letters*. 2012;12(1):402-406.
97. Spesyvtseva SES, Dholakia K. Trapping in a material world. *ACS Photonics*. 2016;3(5):719-736.

98. Gross P, Farge G, Peterman EJ, et al. Combining optical tweezers, single-molecule fluorescence microscopy, and microfluidics for studies of DNA–protein interactions. *Methods in Enzymology*. 2010;475:427-453.
99. Goksör M, Enger J, Hanstorp D. Optical manipulation in combination with multiphoton microscopy for single-cell studies. *Applied Optics*. 2004;43(25):4831-4837.
100. Montag M, Rink K, Delacretaz G, et al. Laser-induced immobilization and plasma membrane permeabilization in human spermatozoa. *Human Reproduction* 2000 Apr;15(4):846-52.
101. Xie C, Dinno MA, Li Y-q. Near-infrared Raman spectroscopy of single optically trapped biological cells. *Optics letters*. 2002;27(4):249-251.
102. Jess P, Garcés-Chávez V, Smith D, et al. Dual beam fibre trap for Raman microspectroscopy of single cells. *Optics Express*. 2006;14(12):5779-5791.
103. Diekmann R, Wolfson DL, Spahn C, et al. Nanoscopy of bacterial cells immobilized by holographic optical tweezers. *Nature Communications*. 2016;7(1):1-7.
104. Kreysing MK, Kießling T, Fritsch A, et al. The optical cell rotator. *Optics Express*. 2008;16(21):16984-16992.
105. Yang Z, Piksarv P, Ferrier DE, et al. Macro-optical trapping for sample confinement in light sheet microscopy. *Biomedical Optics Express*. 2015;6(8):2778-2785.
106. Dholakia K, Drinkwater BW, Ritsch-Marte M. Comparing acoustic and optical forces for biomedical research. *Nature Reviews Physics*. 2020;2(9):480-491.
107. Yang Z, Cole KL, Qiu Y, et al. Light sheet microscopy with acoustic sample confinement. *Nature Communications*. 2019;10(1):1-8.
108. Thalhammer G, Steiger R, Meinschad M, et al. Combined acoustic and optical trapping. *Biomedical Optics Express*. 2011;2(10):2859-2870.

109. Capitanio M, Pavone FS. Interrogating biology with force: single molecule high-resolution measurements with optical tweezers. *Biophysical Journal*. 2013;105(6):1293-1303.
110. Kirkham GR, Britchford E, Upton T, et al. Precision assembly of complex cellular microenvironments using holographic optical tweezers. *Scientific Reports*. 2015;5(1):1-7.
111. Dao M, Lim CT, Suresh S. Mechanics of the human red blood cell deformed by optical tweezers. *Journal of the Mechanics and Physics of Solids*. 2003/11/01;51(11):2259-2280.
112. Favre-Bulle I, Zhang S, Kashchuk A, et al. Optical tweezers bring micromachines to biology. *Optics and Photonics News*. 2018;29(4):40-47.

Figure Legends

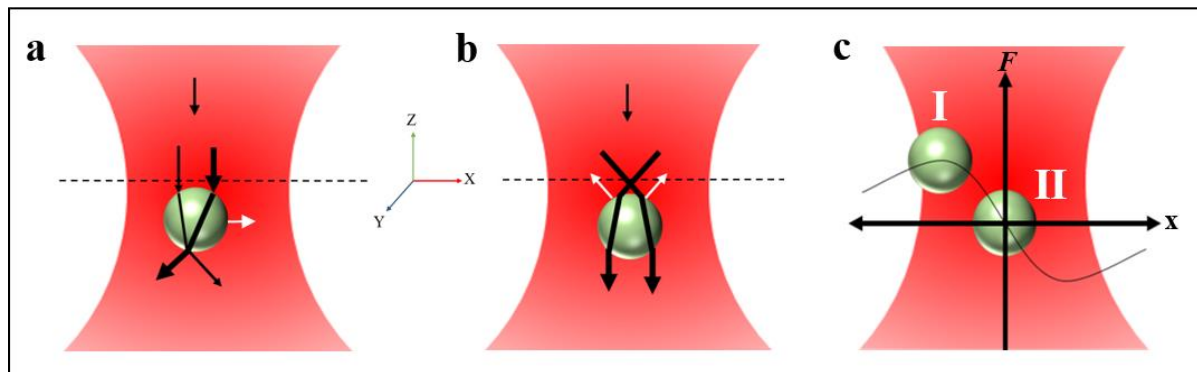


Figure 1. Ray optics model of optical tweezers for a particle of higher refractive index than its surroundings. The beam propagates in the downwards direction as indicated in (a) and (b). The trapped particle is not drawn to scale and only the refraction of the light is shown for simplicity. (a) Lateral Trapping. The particle is maintained in position by optical forces resulting from propagation of the light rays (black lines). The resultant reaction forces (white arrow) act in the x and y directions towards the field maximum. (b) Axial Trapping. The particle finds an equilibrium position on the z-axis by axial momentum (black arrow) and reaction force (white arrow). The particle sits below beam centre (the dashed black horizontal line) as radiation pressure from photon scattering (black arrow) pushes against the particle. The position in the x-y plane is maintained by the intensity gradient of the light field. (c) An overlay of the force versus extension curve for the trapped particle. (c) I shows the particle held at the turnover point of the force extension curve ~ 200 nm away from the trap centre. Here, though trap stiffness is zero, a constant force is exerted. In (c) II the particle is trapped near the centre of the trap and the linear region of force versus displacement is depicted. Displacement of the bead in the x direction results in measurable changes in F.

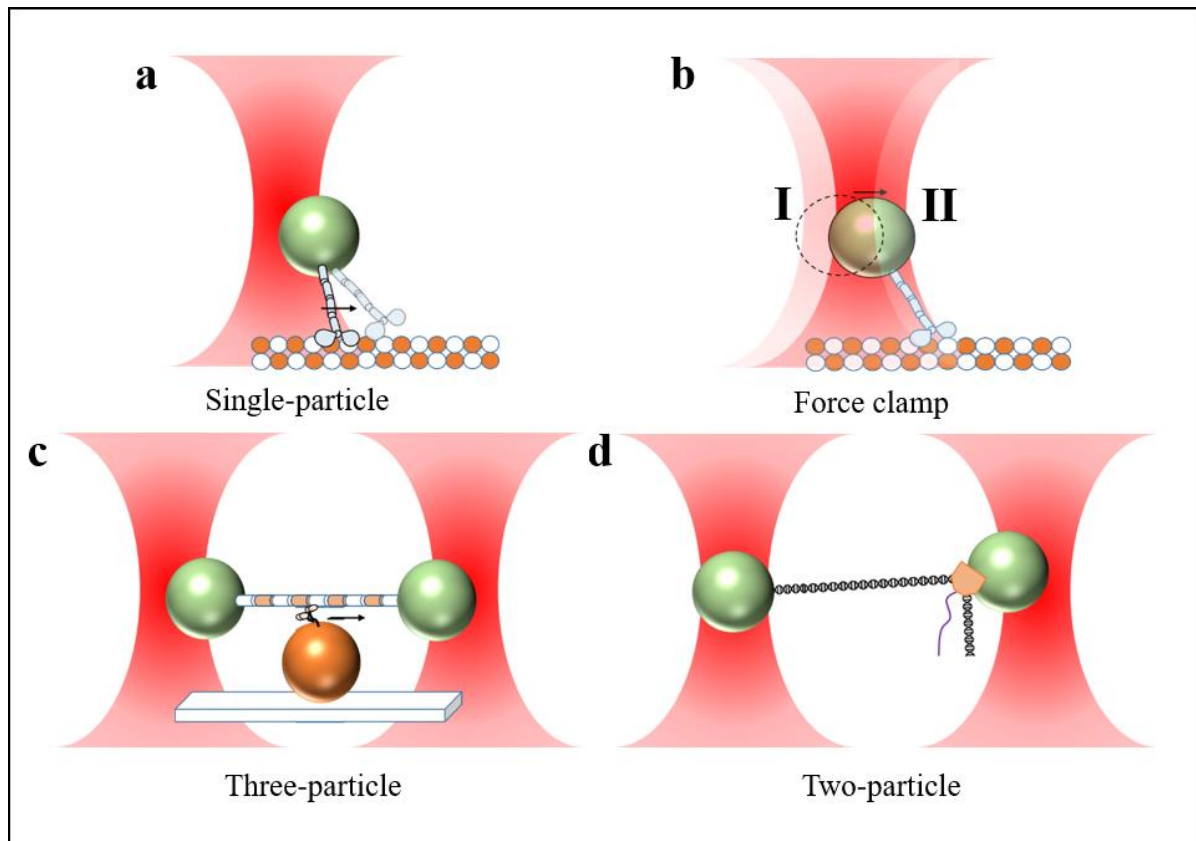


Figure 2. Common optical trapping assays for measuring single molecule forces and displacement as described in Table 1. Particles, laser beams, molecular motors and polymers/microtubules are not drawn to scale. (a) A single-particle assay. The trap is static where particle displacement is reflective of molecular motor displacement. (b) Force clamp. A dynamic trap where the trapping position and force on the particle is maintained. Motion of the particle will accompany trap movement – point I (dotted line) to II (filled line). (c) Three-particle geometry with two static optical traps. Particle displacement on both ends directly represent molecular motor displacement. (d) Two-particle configuration. The left particle is held in a trap of high stiffness. The right particle is positioned at the turnover point as in Figure 1c. This generates a force clamp where displacement at the right particle is accurately reflective of DNA or polymerase activity. Repeating orange and white strands in (a) to (c) represent microtubule or DNA. The black helical strand in (d) represents DNA; the purple strand indicates transcribed RNA. Schematics adapted from [109] and [4].

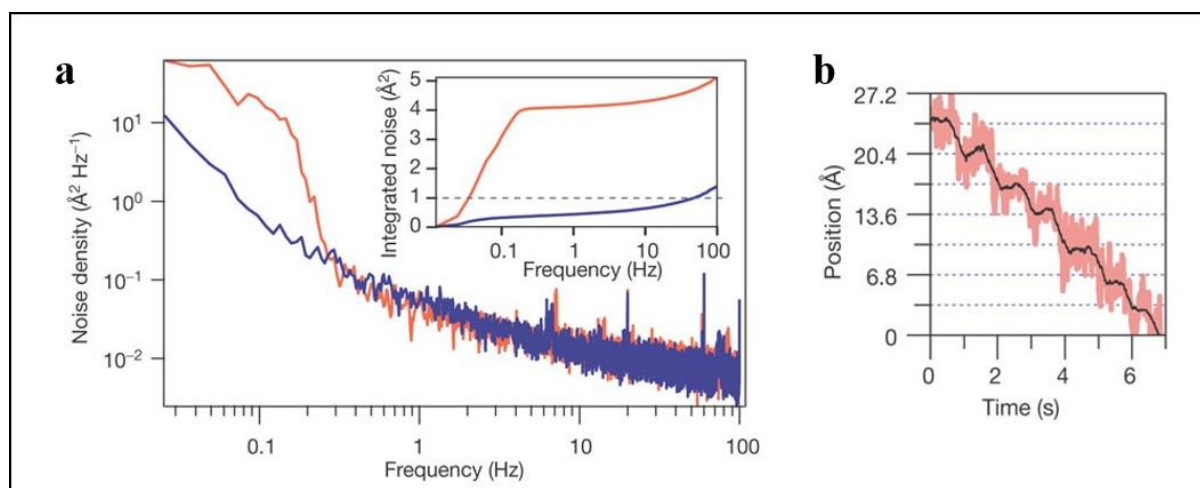


Figure 3. Forces associated with the two bead RNA polymerase optical assay described in Figure 2(d) and used in Abbondanzieri et al. [37]. (a) Power spectrum data for the stiffly trapped bead (left most bead in figure 2 (d)) in air (red) and helium (blue). Inset: the integrated noise spectra for air (red) and helium (blue) shows a tenfold reduction in power. (b) Displacement of resolved RNA polymerase steps in the bead-DNA-bead configuration [37]. Displacement over time is recorded by the right hand (weakly trapped) bead when the stiffly held (leftmost) bead moves in increments of 3.4 \AA at 1 Hz. Data reproduced with permission from [37].

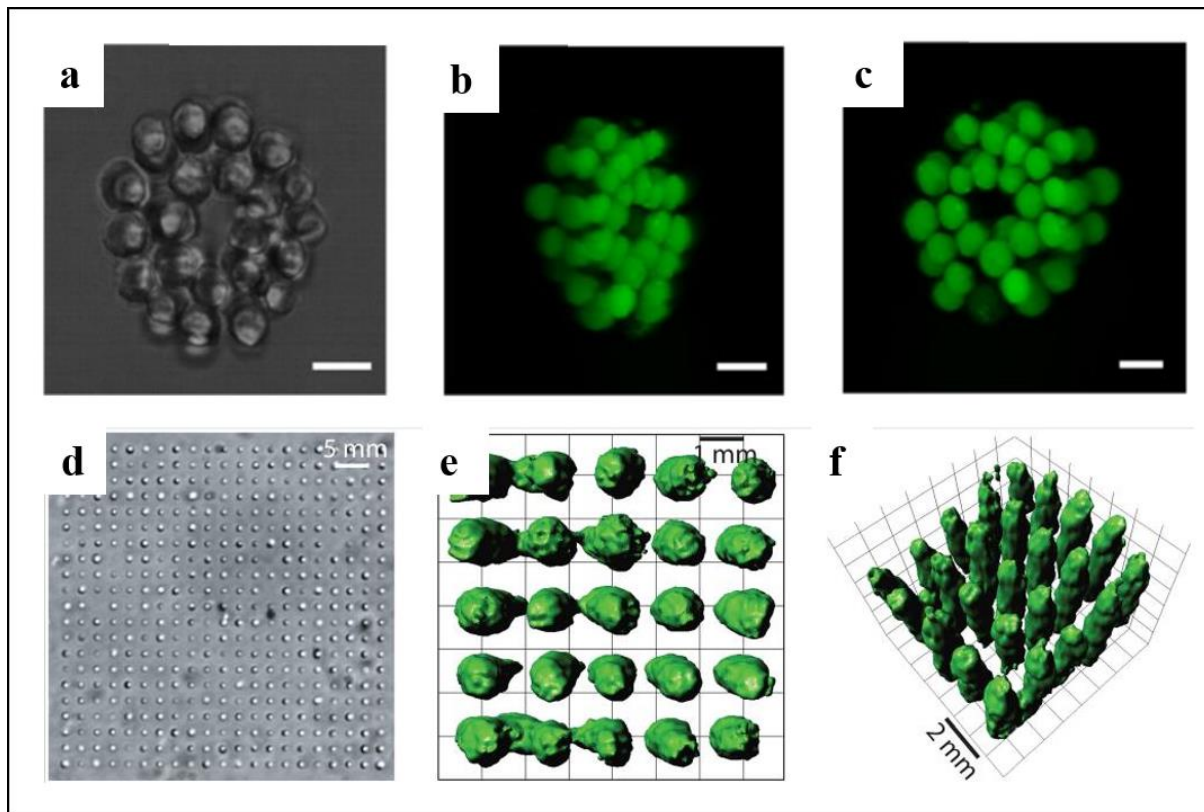


Figure 4. Cell patterning of embryonic stem cells (eSCs) ((a) -(c)) and bacterial cells ((d)-(f)). (a) A brightfield image of eSC organisation using holographic optical tweezers. (b)-(c) Fluorescent confocal images of the cells in (a) showing cell organisation. Scale bar is 12 μm . (d)-(f) Bacterial cell patterning using time multiplexed holographic traps generated by an acousto-optic deflector and spatial light modulator. (d) Micrograph of a 21 x 21 2D custom microarray of *P. aeruginosa* generated through optical manipulation. (e)-(f) By employing a false-colour isosurface in the confocal images, the mean distance between centres of structures is determined as $1.52 \pm 0.06 \mu\text{m}$ with a mean spacing between bacterium of $354 \pm 134 \text{ nm}$. Data in (a)-(c) reproduced with permission from [110] and data in (e)-(f) reproduced with permission from [50].

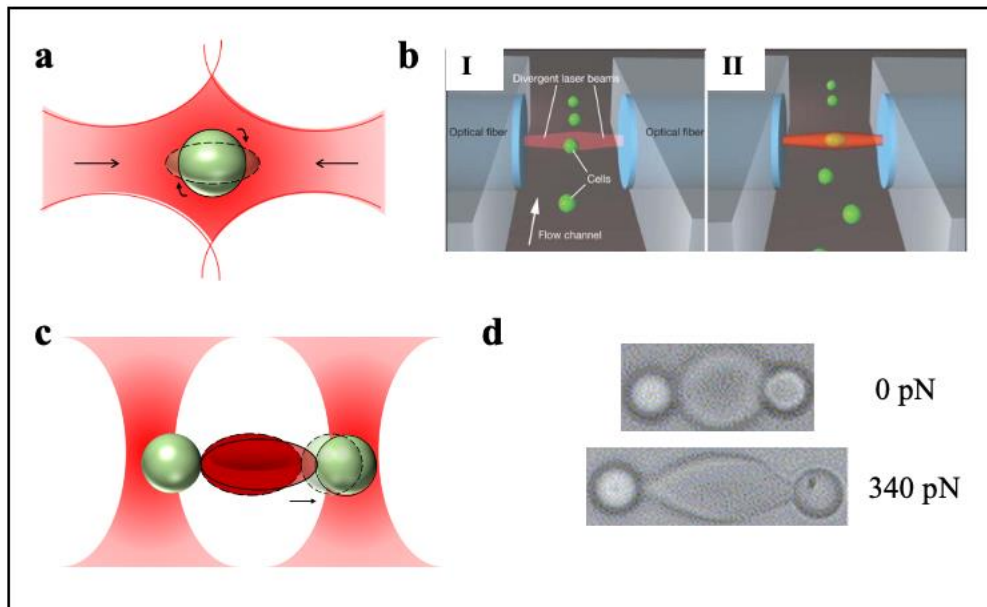


Figure 5. Cell stretching assays in optical manipulation. (a) The counter-propagating dual beam trap acting as a cell stretcher. Two optical beams directed towards each other generate surface forces that enable both trapping and deformation of the cell outwards towards each of the two beams. (b) Optical stretching schematic reproduced with permission from [53]. (b) I Two counter-propagating beams emanating from optical fibres trap cells (green) in a microfluidic flow channel. (b)II Deformation of the trapped cell is induced by typically increasing the laser field. (c) The bead-based cell stretcher. Trapped beads adhered to the surface of the cell act as handles. The left bead is subject to a static trapping force while the right bead (handle) is moved. The deformation of the cell for a given force may be used to determine mechanical characteristics (e.g. shear modulus). (d) Image of the bead-stretching assay on a live red blood cell showing the case of no force (top) vs a force of 340 pN (bottom) is exerted causing stretching. Reproduced with permission from [111].

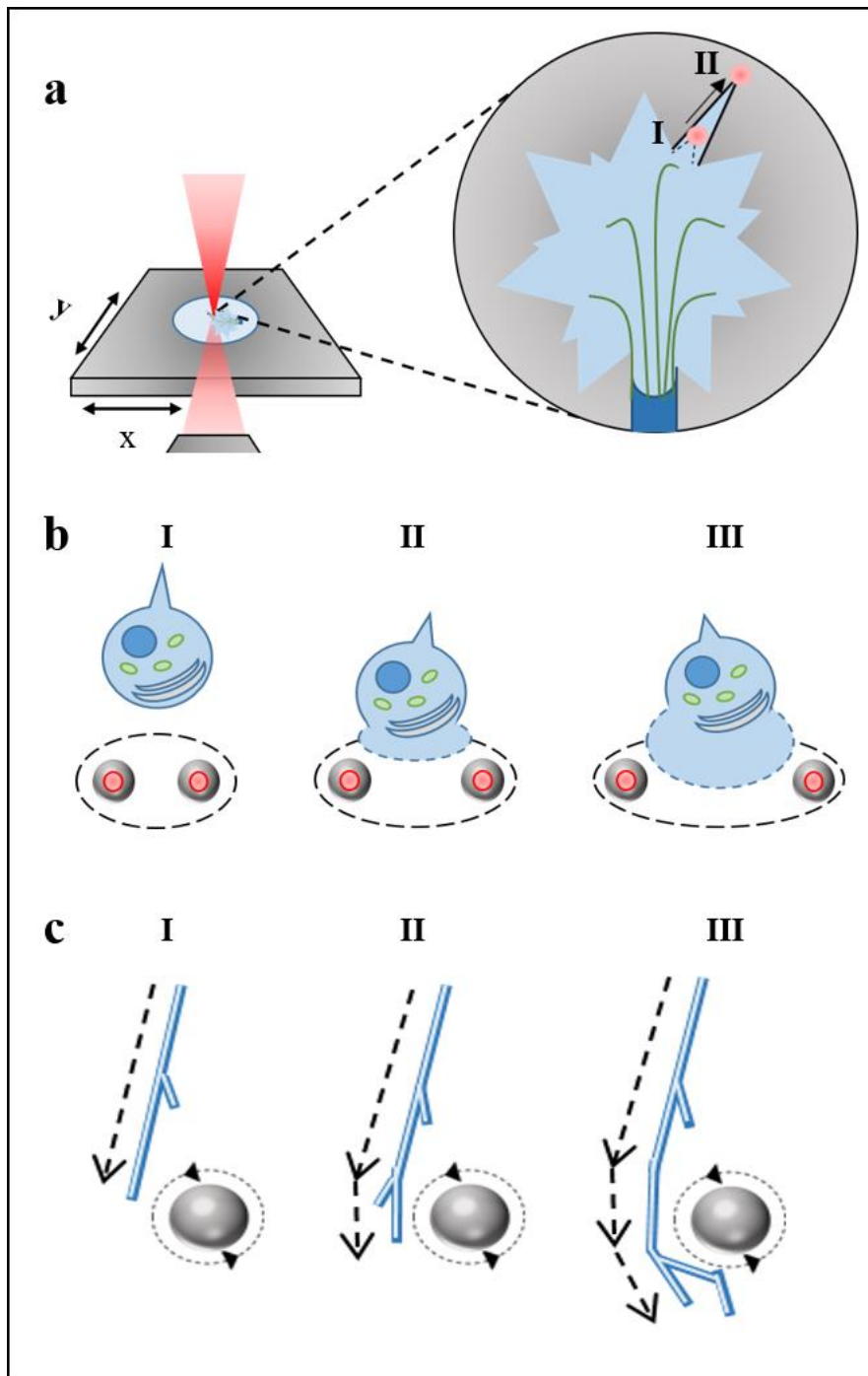


Figure 6. Optical tweezers configurations for guiding cell growth. (a) Single beam assay for the direct guidance of neuronal cell growth (figure adapted from [63]). The laser is directed on an actively developing growth cone at a neuronal edge (position I). Translating the laser at the edge directs guidance of growth (moving the beam from I to II) (b) Indirect guidance of cell growth with optical tweezers through chemotaxis. We see precise positioning and release of a chemoattractant incorporated into a bead (grey) that are held with laser light (red) in the

proximity of leukaemia cells (denoted in blue). Over time the cell develops a lamellipodium (extension) in the direction of the chemoattractant depicted in (b)I to (b)III. Adapted from [66]. (c) Indirect guidance of axon growth, by trapping and rotating a birefringent particle close to an axon. This exerts microfluidic-induced forces on growth cones, resulting in controlled directional axonal growth. In this case an anticlockwise rotating vaterite particle was held adjacent to the axon causing it to change course and follow the rotation of the particle depicted in (c)I-(c)III. Adapted from [67].

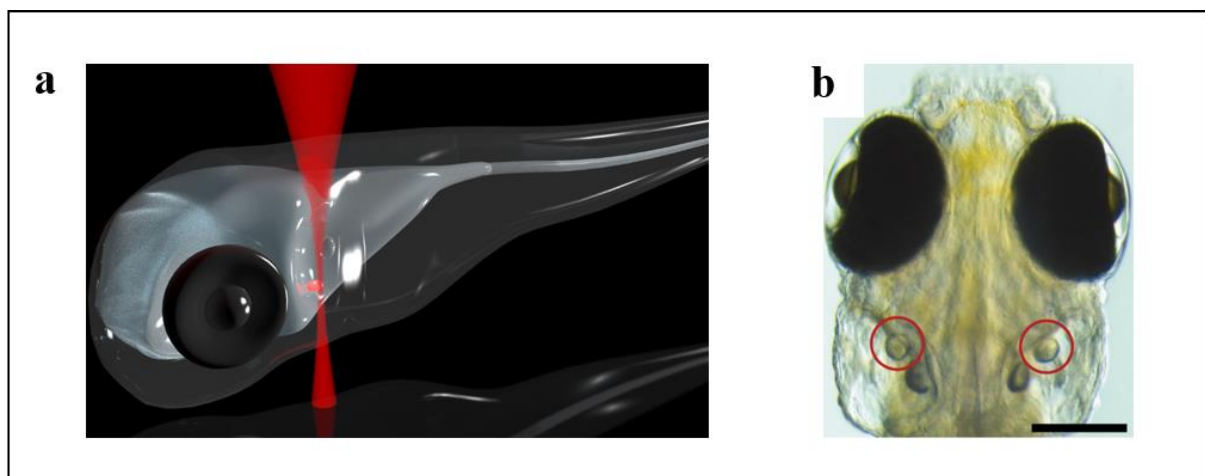


Figure 7. *In vivo* optical trapping of zebrafish otoliths (ear stones). (a) Schematic showing optical trapping of otoliths ($55\ \mu\text{m}$) in zebrafish. Reproduced with permission from [112]. (b) Dorsal view of otoliths (red circles) in a zebrafish larva at 6 days post fertilisation (scale bar denotes $200\ \mu\text{m}$). Reproduced with permission from [73].

| | Optical Tweezers Assay | Configuration | Molecular Motor of Application |
|---------|-----------------------------------|---|--------------------------------|
| Static | Single Bead <i>Figure 2a</i> | bead – molecular motor – polymer chain | Kinesin, RNA polymerase |
| | Three Bead <i>Figure 2c</i> | bead – polymer (molecular motor) – bead | Myosin, Kinesin, Dynein |
| | Two Bead <i>Figure 2d</i> | bead – DNA strand – molecular motor – bead | RNA polymerase |
| Dynamic | Force – Clamp <i>Figure 2b</i> | bead – molecular motor – polymer chain | Kinesin, Dynein |
| | Position – Clamp | bead – polymer chain (molecular motor) – bead | Myosin |

Table Legend

Table 1. Optical Trapping assays and their respective configurations for the measurement of molecular motor displacement. () indicates attachment of molecular motor to polymer. Adapted from references [109] and [4]